Department of Veterans Affairs

Journal of Rehabilitation Research
and Development Vol. 30 No. 2 1993
Pages 224–232

A Technical Note

Characterization of the dynamic stress response of manual and powered wheelchair frames

J. David Baldwin, MS and John G. Thacker, PhD
Rehabilitation Engineering Center, University of Virginia, Charlottesville, VA 22903

Abstract—Two wheelchairs, one manual, one electrically powered, were instrumented with strain gages and operated over various laboratory terrains. Both wheelchairs were folding models with cross tubes pinned together at the center. The wheelchairs were operated on a constant speed treadmill with no bump, and with 0.953 cm (0.375 in) and 1.6 cm (0.625 in) dowels simulating bumps. The wheelchairs were also rolled off a 10.8 cm (4.25 in) platform to simulate a curb drop. The von Mises stresses were computed from the recorded strains, and statistical hypothesis tests were performed to determine whether the stresses were consistent with a stationary, narrow-band Gaussian random process. Such a stress history has been used in random fatigue analyses. Summary data for two strain gage locations on each wheelchair, for the four different test terrains, suggest that the von Mises stress can be considered stationary, but neither narrow-banded, nor Gaussian distributed.

Key words: *dynamic response, manual wheelchair, metal fatigue, power wheelchair, random process, strain gage, treadmill testing.*

INTRODUCTION

Active wheelchair users operate their wheelchairs over many different terrains in the course of their day. The roughness of the terrain and the response of a particular wheelchair structure to that terrain are the controlling factors in several aspects of wheelchair performance, including ride comfort and the long-term survivability of the structure. Long-term survivability of the wheelchair frame is basically an issue of the susceptibility of that frame to metal fatigue, and the accumulation of fatigue damage over the lifetime of the wheelchair. One measure of structural longevity that accounts for the inherent variability in loading, structural response, and material properties, is the probability of failure of the structure.

It was shown by Rice (1) that the peaks of a stationary, narrow-band Gaussian (SNG) random process follow the Rayleigh distribution. Miles (2) first used this result in studying the fatigue of aerospace structures excited by acoustic emissions. If the stresses in a solid are assumed to be adequately modeled by a SNG process, then it follows that the stress peaks are Rayleigh distributed. By coupling a probability distribution of stress peaks with a fatigue model (*S-N* curve), and cumulative damage rule (generally Miner's hypothesis), random fatigue models have been derived from which various statements of the probability of fatigue failure are given (2,3,4,5,6). None of these investigators, however, addressed the task of substantiating the validity of the stress random process assumption for their analyses.

Address all correspondence and requests for reprints to: J.D. Baldwin, PhD, School of Aerospace and Mechanical Engineering, Room 212, Felgar Hall, University of Oklahoma, Norman, OK 73019-0601.

The probability of fatigue failure of a tubular wheelchair frame has been addressed (7,8,9), but purely from the perspective of assumed structural loading. Structural loading and response data for the wheelchair frame under consideration were presumed known. The primary assumption made by Baldwin, et al. (7,8,9) was that the dynamic stresses acting in a wheelchair structural element could be adequately modeled by a SNG random process (at the time no real data for the response of a wheelchair structure under load were available). Then, a probability density function for the number of stress cycles to failure in fatigue was derived following Lambert's method (4).

This study was undertaken to investigate the accuracy of the SNG stress random process model as it applies to specific locations on two wheelchair frames. Dynamic strain gage data were recorded and analyzed for a manual and power wheelchair with a human occupant riding over bumps on a treadmill and performing a simulated curb drop. Statistical hypothesis testing was performed to provide an objective measure of the agreement of the computed von Mises stress data with the SNG assumption. Testing was carried out so that data collection occurred only for one pass of the wheelchair over a given bump, or for one drop from the platform; therefore, the validity of the SNG assumption is addressed only for that event. Summary test data and findings from this testing are presented.

The collection of dynamic strain gage data serves two purposes. First, the data will be used to form an objective assessment of the validity of the SNG assumption for the stresses occurring at specific locations in the wheelchairs under test. Second, the body of strain data will provide the basis for future fatigue life estimates of the wheelchair frame locations investigated. It should be stressed that the results presented here are valid only for the wheelchairs tested, for the specific locations instrumented, and for the test terrain under consideration.

Test Equipment and Procedure

Two wheelchairs, an Invacare Rolls IV (manual), and an Invacare Rolls Arrow (power), were used in this investigation. Both wheelchairs were of the folding type with two steel cross tubes pinned together at the center; the steel alloy was unknown in both cases. The manual wheelchair had solid front and rear tires and chrome-plated frame tubes. The front tires of the manual wheelchair had an outside diameter of about 20 cm (7.9 in), and a radial thickness of about 1.9 cm (0.75 in). The power wheelchair had solid front tires, pneumatic rear tires, and painted frame tubes. The front tires of the power wheelchair had an outside diameter of about 19 cm (7.5 in), and a radial thickness of about 3.8 cm (1.5 in).

The major components of the data acquisition system were an AT&T 6300 personal computer containing a MetraByte DAS16 data acquisition board, Measurements Group model 2120 strain gage conditioners, and low pass filters. The data acquisition system was configured to record three channels of data simultaneously. The data acquisition system is illustrated schematically in **Figure 1**; the strain gage terminal blocks are shown at the left side of the figure. A BASIC language computer program initialized and controlled the data collection and a FORTRAN program performed the data reduction and analysis.

The wheelchairs were instrumented with 3-element rectangular strain gage rosettes (WA-06-060WR-120, Micro Measurements Division, Measurements Group, Inc.). The three elements of the rosette have been designated Gage 1, Gage 2, and Gage 3, as shown in **Figure 2**. Each element of the rosette has a gage length and grid width of 1.5 mm (0.060 in), a nominal resistance of 120 ohms, a gage factor of 2.09, and a transverse sensitivity of +0.5 percent. Rosettes such as these allow full determination of the two-dimensional strain state existing at their point of attachment (10).

Two strain gage rosettes were attached to a cross tube, one on the side of the tube directly adjacent to the center pin, the other on the bottom of the tube lying along the pin. The strain gage wiring terminal blocks are shown schematically to

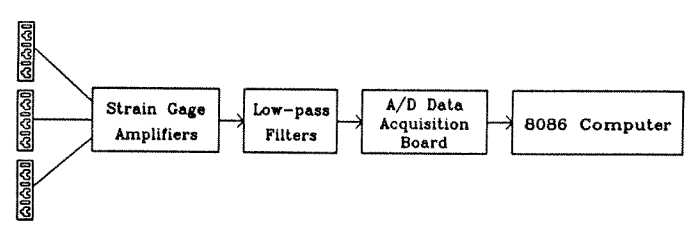

Figure 1.
Schematic representation of data acquisition system.

Journal of Rehabilitation Research and Development Vol. 30 No. 2 1993

indicate the orientation of the gage elements (**Figure 3**). The cross tube was chosen for this initial investigation because several finite element analyses of this type of structure (7,11) have shown that large static stresses occur in this area. The strain gages were installed in the same locations on both the manual and power wheelchairs: they were attached directly to the chrome surface of the manual wheelchair tube. This is a potential source of error in that the strain gages were not attached directly to the base metal. On the power wheelchair, the paint was scraped from the tube at the points of application of the strain gages. The strain gage rosettes have been designated XG1 and XG2 (for "cross tube Gage 1," etc.).

Strain gages measure the average strain over their gage length. If the strain gage is measuring a strain field with large gradients relative to the gage length of the strain gage, an error is introduced into the measurement. For this investigation, it was assumed that the strain gradients at the gage locations were not large with respect to the active length of the strain gages.

Strain gages respond to the deformation of the metal to which they are bonded by a change in their electrical resistance. The change in resistance is measured as a voltage, E, output by a Wheatstone bridge circuit in a "quarter-bridge" configuration (**Figure 4**). The three-wire circuit configuration shown has the advantage of minimizing any temperature variation effects from the data collection (12). The bridge excitation voltage V was nominally 6 volts dc. Each strain gage element had its own Wheatstone bridge circuit.

The strain gages were connected to a bank of strain gage conditioners/signal amplifiers which provided the excitation voltage, bridge calibration and balancing functions, and controlled the amplification of the voltage outputs from the bridge. The signal conditioners had a frequency response of 0–5,000 Hertz ± 5 percent with a gain continuously adjustable from 100 to 2,100 Hz.

The amplified voltage output from each Wheatstone bridge passed through a fourth-order Butterworth active low-pass filter with a nominal signal cutoff at 30 Hz. The low-pass filter acted as a frequency limiter, eliminating elements of the dynamic strain signal that had frequencies larger than the cutoff. This effectively eliminated the electrical noise (typically found at 60 Hz) induced by the

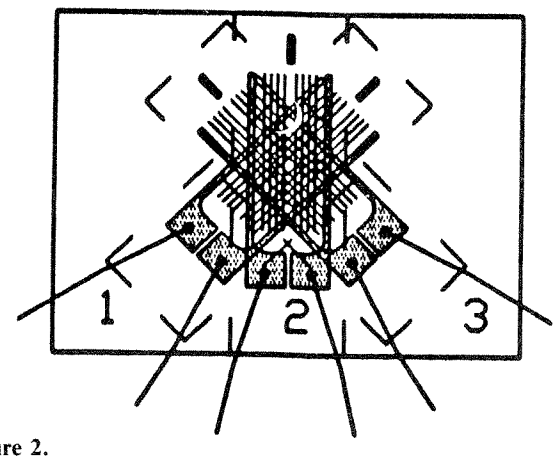

Figure 2.
Rectangular strain gage rosette.

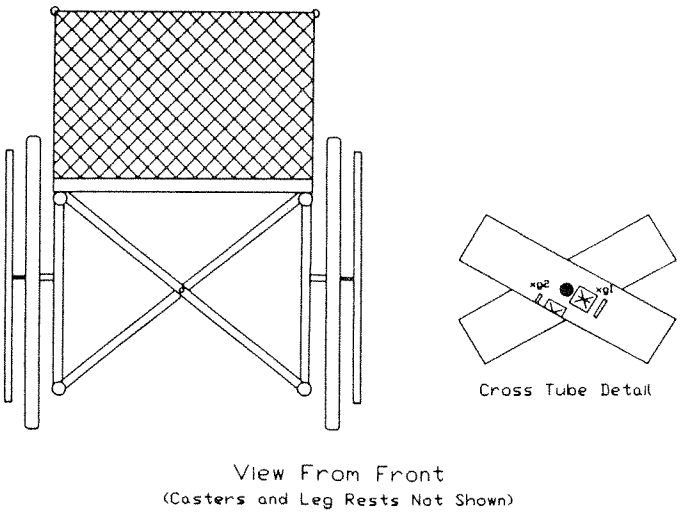

Figure 3.
Location of strain gage rosettes on cross tubes.

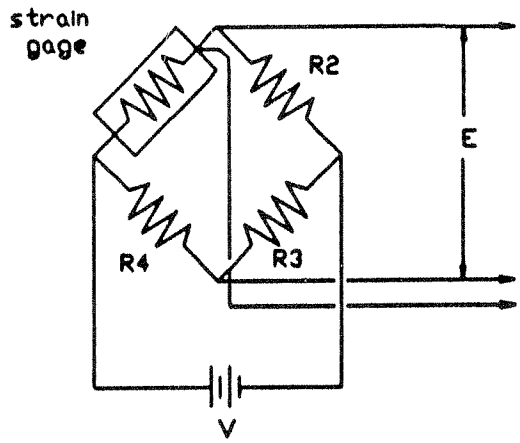

Figure 4.
Wheatstone Bridge circuit.

fluorescent room lighting, nearby power equipment, and miscellaneous atmospheric electrical disturbances. When filtering a signal, one must consider how much data is being thrown away by the filtering process. In this case, unfiltered dynamic strain signals were examined in the frequency domain, and it was found that no significant frequency content existed above about 15 Hz (except a contribution at 60 Hz attributable to lighting). Comparing unfiltered signals to filtered signals showed that more than 98 percent of the unfiltered RMS voltage existed in the filtered data streams; thus, no real data loss occurred due to filtering. It is conceivable, though, that an experimental testing program may excite strains in the wheelchair frame that have higher frequency content, in which case, a different filtering strategy must be used.

The sampling rate for this investigation was set at 512 samples per second from each strain gage channel. This rate was more than ten times the filtered signal bandwidth, allowing accurate detection of the strain wave forms (13) and minimizing the phenomenon of frequency aliasing. Samples were recorded for 4 seconds. This combination of sampling rate and duration produced data streams with an integer power of two number of points, suitable for use in Fourier transform frequency analysis.

The filtered strain signals were sampled by a MetraByte DAS16 analog-to-digital (A/D) data acquisition board mounted in a personal computer. The A/D board was programmed to sample the analog strain signals (voltages) and convert them to digital values suitable for computer storage and manipulation.

To date, both wheelchairs have been tested on both a constant speed treadmill fitted with wooden dowel bumps, and in simulated curb drops. The treadmill testing employed 0.953 cm (0.375 in) and 1.588 cm (0.625 in) diameter bumps, as well as no bump testing. The dowels extended across the width of the treadmill belt and were aligned so that they would be perpendicular to the direction of relative travel of the wheelchair under test. Both front casters impacted the dowels simultaneously. The data collection was initiated manually by the wheelchair occupant and was timed to have the wheelchair impact the bump near the middle of the 4-second data window.

The curb drop test platform simulated a 10.8 cm (4.25 in) drop. The occupied wheelchairs were held in a wheelie position and rolled off the platform. After rear wheel impact, the front casters were allowed to fall to the ground freely. Data collection was triggered manually prior to the wheelchair rolling off the platform.

The treadmill test with no bump was intended to simulate smooth surface operation. The treadmill bump testing was intended to provide data on the response of wheelchairs as they cross obstacles similar to those that might be encountered in everyday operation. The curb drop simulation was from a platform that was not as high as a standard curb, but would nonetheless provide useful data on the response of wheelchairs under rear wheel impact conditions.

A test series involved recording the output of one of the strain gage rosettes on one of the wheelchairs as it traversed one of the test terrains. Thus, for this test program, there were 16 test series; between 5 and 30 data sets were recorded for each test series. For all of the tests reported here, the wheelchair occupant was a nondisabled male with a mass of 80.3 k (177 lbs) and a height of 1.8 m (70 in).

Computational Models

The data processing stage of the investigation required that the recorded digital values be converted to voltages and then to strains. The strains were corrected for the transverse sensitivity of the strain gages (14), and then the mean and standard deviation of each strain gage output data stream were calculated.

The principal strains and stresses were computed from the output of the strain gage rosettes. The principal strains ϵ_1, ϵ_2, and γ_{max} were calculated using the relationships between the strains measured by the rosettes (10):

$$\epsilon_{1,2} = \frac{\epsilon_0 + \epsilon_{90}}{2} \pm \frac{\sqrt{(\epsilon_0 - \epsilon_{90})^2 + [2\epsilon_{45} - (\epsilon_0 + \epsilon_{90})]^2}}{2}$$

$$\gamma_{max} = \sqrt{(\epsilon_0 - \epsilon_{90})^2 + [2\epsilon_{45} - (\epsilon_0 + \epsilon_{90})]^2} \qquad [1]$$

$$\phi = \frac{1}{2} \tan^{-1} \left[\frac{2\epsilon_{45} - (\epsilon_0 + \epsilon_{90})}{\epsilon_0 - \epsilon_{90}}\right]$$

The quantities ϵ_0, ϵ_{45} and ϵ_{90} were the strains measured by Gage 1, Gage 2, and Gage 3 of the rosette, respectively. The angle ϕ measured the angle between the line of Gage 1 and the maximum

Journal of Rehabilitation Research and Development Vol. 30 No. 2 1993

principal strain, ϵ_1. Once the principal strains had been calculated using **Equation 1**, the principal elastic stresses were computed using the plane stress constitutive relationships (15):

$$\sigma_1 = \frac{E}{1-\nu^2}(\epsilon_1 + \nu\epsilon_2)$$

$$\sigma_2 = \frac{E}{1-\nu^2}(\epsilon_2 + \nu\epsilon_1) \qquad [2]$$

$$\tau_{max} = \frac{E}{2(1+\nu)}\gamma_{max}$$

where υ is the Poisson ratio and E is the elastic modulus. For the steel tube material considered here, these parameters were assumed to have the values $\upsilon = 0.285$ and $E = 29.5 \times 10^6$ psi. The quantities σ_1, σ_2 and τ_{max} are the maximum principal stress, minimum principal stress, and maximum shear stress, respectively, in the frame tube at the location of the strain gage. The von Mises stress was computed from the principal stresses using the relationship

$$\sigma_e = \sqrt{\sigma_1^2 + \sigma_2^2 - \sigma_1\sigma_2} \qquad [3]$$

Several statistical hypothesis tests were performed on each data set to determine the agreement of the recorded data with the SNG assumption. The Reverse Arrangements Test for data independence addressed the stationary nature in time of the data stream; in this case, the stationary nature of the mean square value of the data was investigated. A parameter known as the *regularity factor* was computed to determine whether the data exhibited narrow-band behavior. Finally, the chi-square goodness of fit test provided an estimate of the agreement between the measured data and a Gaussian distribution. It was the time variation of the von Mises stress, σ_e, that was examined for consistency with the stationary, narrow-band Gaussian random process assumption.

In order to perform the Reverse Arrangements Test (16,17), the σ_e data stream was divided into 20 intervals. The mean square value was computed for each interval and reverse arrangements were then calculated. The 95 percent confidence interval for the Reverse Arrangements Test with 20 intervals is from 65 to 125 reversals. If the data sample produced less than 65 or more than 125 reverse arrangements, the assumption of stationary data was rejected.

The regularity factor α of the σ_e data stream was calculated to determine whether the data represented narrow-band response. For experimental data, the regularity factor is defined as the number of times a data stream has an upcrossing of its mean value divided by the number of peaks above the mean value (18). The regularity factor can have values in the interval $0 < \alpha < 1$. A regularity factor $\alpha \approx 1$ indicates narrow-band response where nearly every positive peak occurs above the mean value of the data. This situation arises when there is one dominant frequency in the data. When $\alpha \approx 0$, very few of the positive peaks occur above the mean value and wide-band response is indicated. Wide-band response refers to the fact that the frequency content of a signal is spread over a range of frequencies. It is the higher frequency cycles superimposed on the low frequency cycles that lead to peaks below the signal mean value.

Finally, a chi-square goodness of fit test (16) was performed on the σ_e data stream. Using the computed mean and standard deviation, the stresses were compared with a Gaussian distribution having the same mean and standard deviation. The data were grouped into 16 bins 0.4 standard deviations wide ranging from -2.8 to $+2.8$ standard deviations and compared with the expected number of observations assuming a Gaussian distribution. The 95 percent confidence limit for a chi-square test with 13 degrees of freedom is 22.4. If the data sample produced a chi-square statistic greater than 22.4, the assumption of conformance with the Gaussian distribution was rejected.

RESULTS AND DISCUSSION

Because of the volume of data on hand (370 data sets of 6,144 data points each), a complete data presentation will not be given in this paper. However, one data set from one of the manual wheelchair treadmill tests will be examined in detail, and the statistics of several other treadmill and curb drop data sets will be presented.

The data set designated TRD55 is from a 4-second treadmill test on the manual wheelchair, recording strain gage rosette XG1. The treadmill bump was 0.953 cm (0.375 in) in diameter, the

wheelchair occupant was a nondisabled male with a mass of 80.3 k (177 lbs), and the nominal treadmill speed was 1 m/sec. The strain versus time plot of this test is shown in **Figure 5**. The data are plotted in terms of microstrain (= strain * 10^6).

Notice that the strains recorded by Gage 1 were nearly always in compression, while Gage 3 was usually in tension. Gage 2 strains went through both tension and compression in a cyclic fashion. It is also interesting to note that the Gage 2 signal had a wider range between the maximum and minimum strains (~91 microstrain) than either Gage 1 (~39 microstrain) or Gage 3 (~46 microstrain). This was the result of the orientation of the Gage 2 element of the XG1 rosette along the tube axis, as shown in **Figure 3**, tending to measure the overall axial tension and compression of the tube, as well as any bending action out of the plane of the tubes. This observation was not surprising, given that the vertical motions of the wheelchair occupant (caused by the bump) would tend to be transmitted to the cross tube in a predominantly compressive manner. The orientations of Gages 1 and 3 were such that they tended to measure the twisting of the tube, which the data show to be a relatively constant state.

A very noticeable feature of this data set is the rapid variations shown by all three gages in the time interval from approximately 1.5 to 2.0 seconds. This is the time period where the measured strains varied most widely in response to the bump on the treadmill. It can be seen in **Figure 5**, that the Gage 2 strain had large compressive peaks near times 1.5 seconds and 2.0 seconds. These points are about 0.5 seconds apart and represent a spatial separation of approximately 50 cm (19.6 in) at the 1 m/sec treadmill speed. The points of contact of the front and back wheels of the manual wheelchair were about 35.6 cm (14 in) apart. It seems reasonable to assume that the large negative strain peaks seen in the Gage 2 signal at times 1.5 seconds and 2.0 seconds were the response of the wheelchair to the bump impacting the front and rear wheels, respectively. What appears to be another response increase occurred just prior to 3.0 seconds. It is felt that this response was due to the settling of the wheelchair occupant after passing over the bump. These three events are marked with arrows in **Figure 5**.

Given the rosette strain output, the principal stresses were calculated for this test. **Figure 6** shows the maximum principal stress, minimum principal stress, maximum shear stress, and the angle counterclockwise from Gage 1 to the maximum principal stress. All four of these quantities exhibit increased variation during the bump. The figure shows that the rotation angle is typically in the neighborhood of 90°, which is aligned with Gage 3.

It can be seen that the angle to the maximum principal stress ϕ is not constant, but varies with time (**Figure 6**). The implication of this observation is that a biaxial fatigue theory incorporating nonproportional loading (i.e., variable angle to maximum principal stresses) should be considered when designing such a connection for fatigue. Also, like the strains, the principal stresses exhibited larger than average variations in the time intervals near 1.5–2.0 seconds and 3.0 seconds.

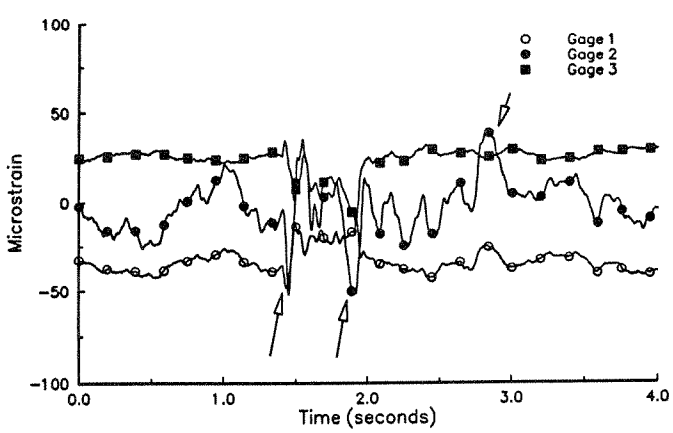

Figure 5.
Strain vs. time history for a treadmill test.

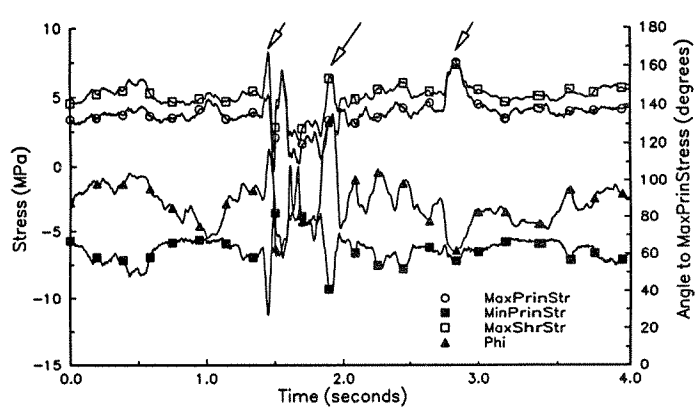

Figure 6.
Principal stresses and angle for a treadmill test.

Journal of Rehabilitation Research and Development Vol. 30 No. 2 1993

The von Mises stress history was computed using **Equation 3** and is plotted in **Figure 7**. As with the strains and principal stresses, the von Mises stress exhibits increased variation in the time intervals near 1.5–2.0 seconds and 3.0 seconds.

The Reverse Arrangements Test for the TRD55 σ_e data stream yielded 81 reverse arrangements, indicating that the mean square von Mises stress was stationary in time. The σ_e regularity factor α was found to be 0.129, indicative of wide-band variations. Thus, the narrow-band assumption was rejected for this data set. The calculated chi-square measure was 1,082, which was large enough to cause rejection of the Gaussian distribution hypothesis.

The TRD55 chi-square, reverse arrangements, and regularity factor numbers were typical of the other data sets. Summary test data for both the manual and powered wheelchair treadmill tests is presented in **Table 1**. A similar summary of data from the curb drop simulations is presented in **Table 2**. The data sets chosen for analysis were considered to be representative of the body of test data. The data in **Table 1** and **Table 2** show that for most of the test data presented, the null hypothesis that the von Mises stresses are stationary could not be rejected. All of the tabulated data exhibit wide-band behavior (i.e., $\alpha \ll 1.0$). Finally, a most notable result is that none of the tests were even close to satisfying the Gaussian assumption. It is felt that this is due to the highly correlated (in time) nature of the deformations in a structure as it vibrates. The Gaussian distribution presumes independent data points. It appears that any sampling of structural

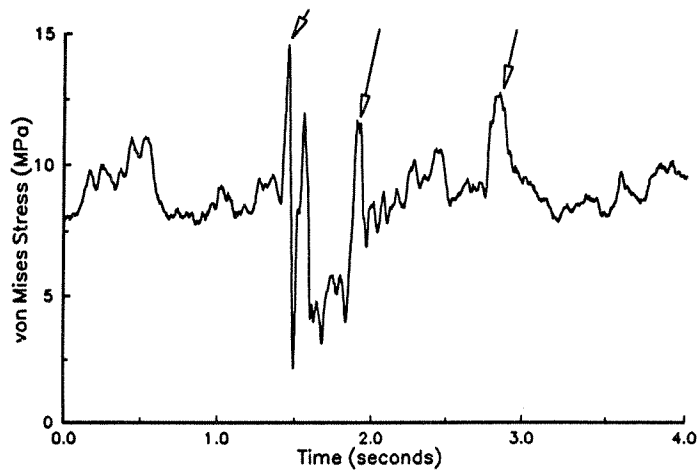

Figure 7.
Von Mises stress for a treadmill test.

Table 1.
Summary treadmill test data.

Test Index	Wheelchair	Gage	Bump Diam. (cm/in)	von Mises Stress Rev. Arr.	α	χ^2
10	Manual	XG2	0.0/0.0	25	0.026	1466
30	"	XG1	0.0/0.0	69	0.126	171
55	"	XG1	0.953/0.375	81	0.129	1082
80	"	XG2	0.953/0.375	38	0.036	1110
115	"	XG2	1.59/0.625	107	0.070	4750
145	"	XG1	1.59/0.625	85	0.212	957
195	Power	XG1	0.0/0.0	86	0.143	136
215	"	XG2	0.0/0.0	54	0.182	178
250	"	XG2	0.953/0.375	47	0.214	796
270	"	XG1	0.953/0.375	100	0.377	655
305	"	XG1	1.59/0.625	92	0.168	655
330	"	XG2	1.59/0.625	107	0.192	1935

Table 2.
Summary curb drop test data.

			von Mises Stress		
Test Index	**Wheelchair**	**Gage**	**Rev. Arr.**	α	χ^2
3	Manual	XG1	119	0.343	2344
7	"	XG2	112	0.045	1524
12	Power	XG1	61	0.300	4111
18	"	XG2	145	0.024	4066

responses, such as strains, that occurs at a rate high enough to capture the peaks of the signal, will result in data points that are too strongly correlated to be accurately modeled by a Gaussian distribution.

The frequency content of the dynamic strains is displayed in **Figure 8**, which shows the magnitude of the Fourier transform of the strain data from each gage of the rosette. It was stated earlier that the frequency content of the strain data was confined to the lower frequencies; this is demonstrated in **Figure 8**. The low frequency content of the strains extended to the von Mises stresses also (**Figure 9**). It can be seen from **Figure 9** that the frequency content of the von Mises stress extends beyond the large component at 0 Hz. The band of frequency components above 0 Hz is graphical indication that the narrow-band assumption is not satisfied.

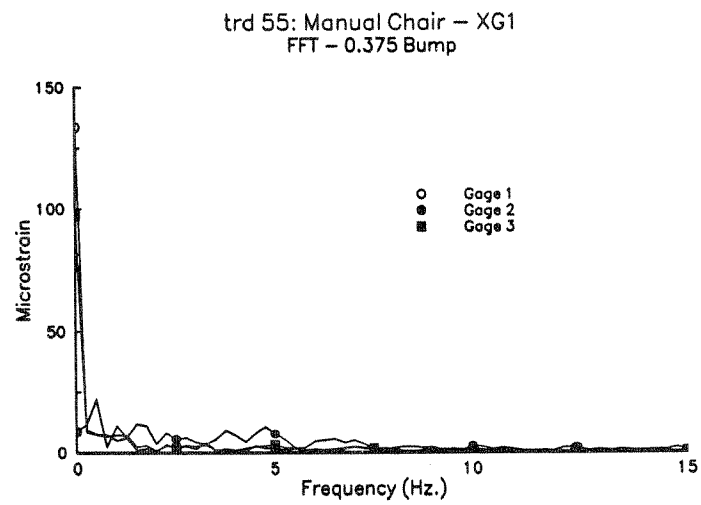

Figure 8.
Frequency content of strain data.

CONCLUSIONS

The test program described here has been useful in demonstrating the time-varying nature of the dynamic strains and stresses in a wheelchair cross tube. The implementation of a data collection and analysis system has allowed the examination of the dynamic response of wheelchair frames and the nature of the deformations that cause metal fatigue. Specifically, the assumption that the dynamic von Mises stresses developed in the manual wheelchair, impacting a 0.953 cm (0.375 in) treadmill bump, are narrow-band and Gaussian distributed at the cross tube location investigated, does not appear to be valid. The data did indicate, however, that the von Mises stress response could be taken to be stationary during the bump. Data have been presented for other wheelchair/strain gage location/terrain combi-

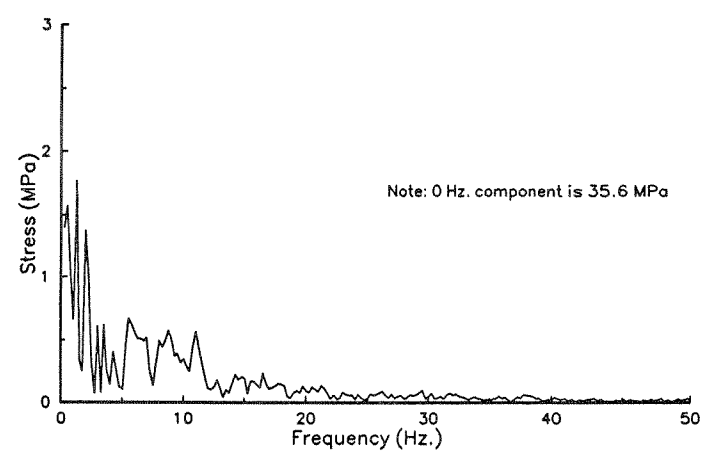

Figure 9.
Fourier transform magnitude of von Mises stress.

nations that lead to the same conclusions. One should remember, however, that other wheelchair/location/terrain combinations may exhibit the assumed narrow-band Gaussian response, although this outcome seems unlikely due to the correlation in time of the deformations of a vibrating structure.

It has also been shown that the computed principal stresses tend to change directions during the traverse of a bump. Such behavior may indicate that a biaxial fatigue analysis is required when analyzing the probability of failure of joints such as those investigated here.

The data and findings presented here are for a very small fraction of the possible wheelchair frame locations and load conditions that may be examined. It is not to be inferred from these findings that the von Mises stress in a dynamically loaded wheelchair frame can generally be considered stationary, but neither narrow-band nor Gaussian distributed. Similarly, the frequency spectra presented can be considered valid only for the specific test configuration used here.

In the future, effort will be made to implement fatigue analysis procedures that take advantage of the recorded strain signals to develop estimates of the time-to-failure of dynamically loaded wheelchair frames. Also, testing could be expanded to explore the effect of different test terrains, investigate other high stress wheelchair frame locations, and other types of wheelchair structures.

ACKNOWLEDGMENTS

This work was carried out at the University of Virginia Rehabilitation Engineering Center. The authors are pleased to acknowledge the support provided under NIDRR Grant Number H133E80003.

REFERENCES

1. Rice SO. Mathematical analysis of random noise. Bell systems technical journal. 1944:23:282-322; 1945:24:46-156.
2. Miles JM. On structural fatigue under random loading. J Aeronaut Sc Nov 1954:753-62.
3. Crandall SH, Mark WD, Khabbaz GR. The variance in Palmgren-Miner damage due to random vibration. In: Proceedings of the fourth U.S. National Congress of Applied Mechanics, 1962:119-26.
4. Lambert RG. Analysis of fatigue under random vibration. Shock Vibration Bull Aug 1976:55-71.
5. Shin YS, Lukens RW. Probability based high cycle fatigue life predictions. In: Shin YS, Au-Yang MK, eds. Random fatigue life prediction, PVP-Vol 72. New York: American Society of Mechanical Engineers, 1983:73-87.
6. Wirsching PH, Haugen EB. Probabilistic design for random fatigue loads. J Eng Mech Div 99(EM6):Dec 1973:1165-79.
7. Baldwin JD. Structural reliability analysis of power wheelchair frames. (Thesis). Charlottesville, VA: University of Virginia, 1990.
8. Baldwin JD, Thacker JG. Structural reliability techniques applied to tubular wheelchair frames. In: Proceedings of the 14th annual RESNA conference. Washington, DC: RESNA Press, 1991:237-9.
9. Baldwin JD, Thacker JG, Baber TT. Estimation of structural reliability under random fatigue conditions. In: Service TH, ed. Reliability, stress analysis and failure prevention. New York: American Society of Mechanical Engineers, 1991:43-8.
10. Perry CC, Lissner HR. The strain gage primer. New York: McGraw-Hill, 1962.
11. Disher TD. Stress analysis of three wheelchair frames. (Thesis). Charlottesville, VA: University of Virginia, 1986.
12. Dally JW, Riley WF. Experimental stress analysis, 3rd ed. New York: McGraw-Hill, 1991.
13. Scott K, Owens A. Instrumentation. In: Window AL, Hollister GS, eds. Strain gage technology. London: Applied Science Publishers, 1982.
14. Errors due to transverse sensitivity in strain gages. (Bulletin TN-509). Raleigh, NC: Measurements Group, Inc., 1982.
15. Timoshenko SP, Goodier JN. Theory of elasticity. 3rd ed. New York: McGraw-Hill, 1970.
16. Bendat JS, Piersol AG. Random data: analysis and measurement procedures. 2nd ed. New York: John Wiley & Sons, 1986.
17. Kendall MG, Stuart A. The advanced theory of statistics. Volume II: inference and relationship. 3rd ed. New York: Hafner Publishing Company, 1973.
18. Thoft-Christensen P, Baker MJ. Structural reliability theory and its applications. New York: Springer-Verlag, 1982.